AD-A191 393 A COMPARISON OF VARIOUS ALKALI GAS CELL ATOMIC FREQUENCY STANDARDS. (U) AEROSPACE CORP EL SEGUNDO CA CHEMISTRY AND PHYSICS LAB J C CAMPARO ET AL. 12 FEB 88 TR-0086(6945-05)-5 SD-TR-88-32 1/1

UNCLASSIFIED F/G 14/2 NL

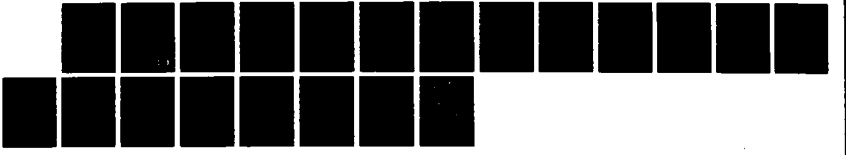

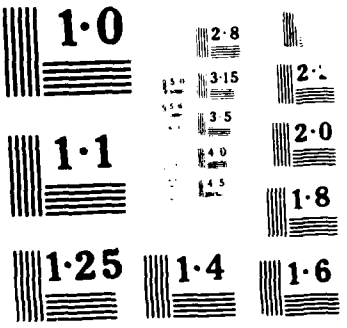
1·0
1·1
1·25
1·4
1·6
1·8
2·0
2·8
3·15
3·5
4·0
4·5

(4)

REPORT SD-TR-88-32

DTIC FILE COPY

AD-A191 393

A Comparison of Various Alkali Gas Cell Atomic Frequency Standards

J. C. CAMPARO and R. P. FRUEHOLZ
Chemistry and Physics Laboratory
The Aerospace Corporation
El Segundo, CA 90245

12 February 1988

Prepared for

SPACE DIVISION
AIR FORCE SYSTEMS COMMAND
Los Angeles Air Force Base
P.O. Box 92960, Worldway Postal Center
Los Angeles, CA 90009-2960

APPROVED FOR PUBLIC RELEASE;
DISTRIBUTION UNLIMITED

DTIC
ELECTE
APR 04 1988
S D
H

88 4 4 117

This report was submitted by The Aerospace Corporation, El Segundo, CA 90245, under Contract No. F04701-85-C-0086 with the Space Division, P.O. Box 92960, Worldway Postal Center, Los Angeles, CA 90009-2960. It was reviewed and approved for The Aerospace Corporation by S. Feuerstein, Director, Chemistry and Physics Laboratory.

Lt Michael J. Mitchell was the project officer for the Mission-Oriented Investigation and Experimentation (MOIE) Program.

This report has been reviewed by the Public Affairs Office (PAS) and is releasable to the National Technical Information Service (NTIS). At NTIS, it will be available to the general public, including foreign nationals.

This technical report has been reviewed and is approved for publication. Publication of this report does not constitute Air Force approval of the report's findings or conclusions. It is published only for the exchange and stimulation of ideas.

Michael J. Mitchell

MICHAEL J. MITCHELL, Lt, USAF
MOIE Project Officer
SD/CWNZS

Raymond M. Leong

RAYMOND M. LEONG, Major, USAF
Deputy Director, AFSTC West Coast Office
AFSTC/WCO OL-AB

UNCLASSIFIED
SECURITY CLASSIFICATION OF THIS PAGE

REPORT DOCUMENTATION PAGE

1a. REPORT SECURITY CLASSIFICATION Unclassified	1b. RESTRICTIVE MARKINGS
2a. SECURITY CLASSIFICATION AUTHORITY	3. DISTRIBUTION / AVAILABILITY OF REPORT Approved for public release; distribution unlimited.
2b. DECLASSIFICATION / DOWNGRADING SCHEDULE	
4. PERFORMING ORGANIZATION REPORT NUMBER(S) TR-0086(6945-05)-5	5. MONITORING ORGANIZATION REPORT NUMBER(S) SD-TR-88-32
6a. NAME OF PERFORMING ORGANIZATION The Aerospace Corporation Laboratory Operations 6b. OFFICE SYMBOL (If applicable)	7a. NAME OF MONITORING ORGANIZATION Space Division Los Angeles Air Force Base
6c. ADDRESS (City, State, and ZIP Code) El Segundo, CA 90245	7b. ADDRESS (City, State, and ZIP Code) Los Angeles, CA 90009-2960
8a. NAME OF FUNDING / SPONSORING ORGANIZATION 8b. OFFICE SYMBOL (If applicable)	9. PROCUREMENT INSTRUMENT IDENTIFICATION NUMBER F04701-85-C-0086-P00016
8c. ADDRESS (City, State, and ZIP Code)	10. SOURCE OF FUNDING NUMBERS PROGRAM ELEMENT NO. / PROJECT NO. / TASK NO. / WORK UNIT ACCESSION NO

11. TITLE (Include Security Classification)

A Comparison of Various Alkali Gas Cell Atomic Frequency Standards

12. PERSONAL AUTHOR(S)

Camparo, J. C. and Frueholz, R. P.

13a. TYPE OF REPORT	13b. TIME COVERED FROM ____ TO ____	14. DATE OF REPORT (Year, Month, Day)	15. PAGE COUNT
		1988 February 12	17

16. SUPPLEMENTARY NOTATION

17. COSATI CODES			18. SUBJECT TERMS (Continue on reverse if necessary and identify by block number)
FIELD	GROUP	SUB-GROUP	Optical pumping Alkali isotopes Hyperfine polarization

19. ABSTRACT (Continue on reverse if necessary and identify by block number)

In this study a theoretical comparison among various alkali gas cell atomic frequency standards is undertaken, specifically: Rb^{85}, Rb^{87}, Cs^{133}, Cs^{135} and Cs^{137}. It is found that Rb^{87} exhibits the best potential shot-noise-limited performance of all the candidate alkalies (in a minimum volume TE_{111} microwave cavity $\sigma_y(\tau) \approx 5.4 \times 10^{-15}/\sqrt{\tau}$), and that this is due to: 1) a large ground-state hyperfine splitting, and 2) a low value of nuclear spin. Additionally, the calculations indicate the importance of microwave cavity geometry on the stability one can attain with a gas cell atomic frequency standard.

20. DISTRIBUTION / AVAILABILITY OF ABSTRACT	21. ABSTRACT SECURITY CLASSIFICATION
☒ UNCLASSIFIED/UNLIMITED ☐ SAME AS RPT ☐ DTIC USERS	Unclassified
22a. NAME OF RESPONSIBLE INDIVIDUAL	22b. TELEPHONE (Include Area Code) / 22c. OFFICE SYMBOL

DD FORM 1473, 84 MAR — 83 APR edition may be used until exhausted. All other editions are obsolete.

SECURITY CLASSIFICATION OF THIS PAGE

UNCLASSIFIED

CONTENTS

TABLES

Accession For
NTIS GRA&I
DTIC TAB
Unannounced
Justification
By
Distribution/
Availability Codes
Avail and/or
Dist Special
A-1

I. INTRODUCTION

Though gas cell atomic frequency standards based on various alkalies have been discussed in the past (Refs. 1-5), notably the Cs^{133} gas cell standard [3][4], none has ever come near to rivalling the popularity of the Rb^{87} gas cell standard. Obviously, there are several factors which contribute to this situation; for example, Rb^{87} has the second largest ground-state hyperfine splitting of all the stable alkali isotopes (implying a relatively high atomic Q), and it has a low value of nuclear spin I so that optical pumping is relatively efficient in populating the $m_F = 0$ state. The primary reason for the supremacy of the Rb^{87} standard, though, lies with the fortuitous overlap of Rb^{85} and Rb^{87} optical absorption lines, which allows for the construction of a very simple and efficient hyperfine filter for optical pumping with alkali discharge lamps (Ref. 6). However, with the advent of narrowband lasers for optical pumping in atomic frequency standards (Refs. 7, 8), especially single-mode diode lasers (Ref. 9), the prerequisite of an efficient hyperfine filter in the design of a gas cell standard has been eliminated. This in turn has diminished the intrinsic attractiveness of a Rb^{87} gas cell standard. In particular, given the 35% greater ground state hyperfine splitting of Cs^{133}, one must seriously question the relative merits of a rubidium standard in the absence of a hyperfine filter requirement. In the present study it is therefore our desire to theoretically explore the shot-noise limited performance of various laser pumped alkali gas cell standards, so that their intrinsic performance capabilities can, to a degree, be assessed.

Considering the fact that there are very many alkali isotopes with various values of nuclear spin and various ground state hyperfine splittings, it is necessary to reduce this host of candidate gas cell standards by requiring the candidate alkali isotope to possess a few reasonable characteristics. Obviously, the first requirement is that the alkali isotope be either stable or long lived. Specifically, we must require that the isotope have a half-life greater than ten years. This is particulary

important for space applications of frequency standards, where longevity is of prime importance. Furthermore, if major redesign of the standard is to be avoided, the alkali isotope must have half-integer nuclear spin, so that the standard can be based on a field insensitive 0-0 transition (Ref. 10). Thus, considering a full range of alkali isotopes (Ref. 11), one is left with the series of nine candidate alkalies listed in Table I. Additionally, in order to obtain efficient laser pumping, one would require that the hyperfine resonances be well resolved optically, that is, that the Doppler broadening be less than the ground-state hyperfine splitting. Consequently, out of the host of original candidate alkalies, only the following five will be considered for further comparison (Ref. 12): Rb^{85}, Rb^{87}, Cs^{133}, Cs^{135} and Cs^{137}.

Table I. Some Properties of the Candidate Alkali Isotopes.

ALKALI	NUCLEAR SPIN I	% ABUNDANCE OR HALF-LIFE	DOPPLER BROADENING (MHz)*	HYPERINE SPLITTING (MHz)
^{7}Li	3/2	92.58%	2340	804
^{23}Na	3/2	100%	1470	1772
^{39}K	3/2	93.10%	870	462
^{41}K	3/2	6.88%	850	254
^{85}Rb	5/2	72.15%	580	3036
^{87}Rb	3/2	27.85%	570	6835
^{133}Cs	7/2	100%	420	9193
^{135}Cs	7/2	3×10^{6} yr	420	9724
^{137}Cs	7/2	30.0 yr	420	10,116

*Calculated Assuming a Vapor Temperature of 100°C

II. OVERVIEW OF THE GAS CELL FREQUENCY STANDARD MODEL AND CALCULATION

In previous publications (Refs. 13, 14) we have discussed a non-empirical model of the gas cell atomic frequency standard. Based on a specific gas cell geometry, the model calculates the standard's anticipated frequency stability in terms of the positive value of the square root of the Allan variance, the quantity we refer to as the "Allan deviation." Calculation of the amount of optical pumping radiation transmitted through the atomic vapor storage cell as a function of injected microwave signal frequency, yields an atomic hyperfine lineshape. The derivative of this lineshape is proportional to the "error signal" upon which the operation of the standard is based (Refs. 1-5). For these calculations, the only noise source considered is the shot noise generated at the photodiode used to detect the transmitted light. This noise is considered the principal limitation to gas cell standard short-term frequency stability. Its exclusive consideration not only leads to accurate performance modelling, but also results in a consistent estimate of the performance of all the potential standards that are analyzed. To perform the analysis, the model considers the relevant gas phase physics as occurring on two different scales. On what we term the "microscopic scale" the 0-0 hyperfine transition lineshape of an arbitrary alkali atom of half-integer nuclear spin is determined by the generalized Vanier theory of alkali atom hyperfine optical pumping (Refs. 15, 16). Among other parameters, this theory considers the dependence of the hyperfine lineshape on optical pumping light intensity and microwave Rabi frequency. However, because the buffer gas pressure in a gas cell standard effectively freezes the alkali atoms in place on time scales of the order of a Rabi period (Ref. 17), and because the alkali vapor is not necessarily optically thin; these two parameters, and hence the microscopic lineshape, vary from atom to atom within the vapor. Furthermore, as a result of diffusion to the resonance cell walls, where the atoms immediately depolarize on impact, there is a spatial distribution of hyperfine polarization $\langle \hat{I} \cdot \hat{S} \rangle$. In one sense, this spatial distribution of $\langle \hat{I} \cdot \hat{S} \rangle$ can be imagined as being superimposed on the microscopic physics. Thus, there is also a "macroscopic scale" of physics in the problem which is related to the

spatial variation of: (a) the optical pumping light intensity, (b) the microwave Rabi frequency, and (c) $\langle \vec{I} \cdot \vec{S} \rangle$ as a result of diffusion to the resonance cell walls.

In order to treat this macroscopic scale of physics in a reasonably lucid manner, the problem is reduced to one dimension, so that only the longitudinal variation of the optical pumping rate and microwave field strength is considered. This is reasonable because the microwave field can be made uniform in the transverse dimension by dielectrically loading the cavity (Ref. 18), and because the laser intensity can easily be made uniform across the face of the resonance cell. The microwave Rabi frequency distribution along the axial dimension is determined by the microwave cavity mode, assuming that the atomic resonance cell fills the microwave cavity. The axial variation of the optical pumping light intensity is determined by computing a "global" optical pumping parameter ζ in a self-consistent manner. In essence, this global optical pumping parameter determines the fractional population in the optically absorbing hyperfine multiplet, and thus the optical depth of the vapor as a result of optical pumping. Since the model assumes that the alkali atoms are effectively frozen in place in the resonance cell, the first order change in transmitted light intensity as a function of microwave Rabi frequency, for a uniform slice of vapor of thickness dz, depends on the local values of the optical pumping light intensity and microwave Rabi frequency. In order to include the effect of axial diffusion, this first order macroscopic solution is multiplied by the envelope function f(z), which describes the axial distribution of hyperfine polarization in an optically thin vapor. (This procedure for treating diffusion is discussed more fully in Ref. 13.) When considering optical pumping with lamps, where the relative optical pumping rates are typically low, it is fair to approximate f(z) by Minguizzi et al.'s first order diffusion mode (Ref. 19)

$$f(z) = \sin(\pi z/L), \tag{1}$$

where L is the length of the resonance cell. However, as previously discussed (Ref. 14), when the optical pumping light source is a laser, the envelope

function must be generalized so as to be valid for arbitrary optical pumping rates

$$f(z) = \frac{[1 - \exp(-\alpha Z)]\,[\exp(\alpha L) - \exp(\alpha Z)]}{[1 - \exp(-\alpha L/2)]\,[\exp(\alpha L) - \exp(\alpha L/2)]} \qquad (2)$$

In the present analysis, we consider an alkali gas cell atomic frequency standard operating in its traditional configuration (i.e., cw optical pumping), except that the typical rf discharge lamp used for optical pumping is replaced by a single-mode laser tuned to the D_2 optical absorption resonance of the alkali [$n^2P_{3/2} - n^2S_{1/2}(F=I+1/2)$]. Furthermore, we assume that there is no filter cell, and that the resonance cell contains a pure isotopic vapor of the alkali under consideration. The calculations are performed in such a way that, for a particular incident laser intensity, we calculate the resonance cell temperature and peak microwave Rabi frequency that minimize the shot-noise-limited Allan variance as well as the minimum Allan variance value itself. Temperature enters the calculations through: 1) the temperature sensitivity of the alkali's diffusion coefficient, 2) the collision frequency of the alkali atoms (i.e., the relative speed of the atoms), and 3) the alkali vapor number density which determines both the spin exchange rate and the vapor's optical depth. Additionally, we consider a clock operating with a TE_{111} cylindrical microwave cavity of minimum volume

$$L = c\sqrt{3}/2\nu_o \qquad (3a)$$

$$R = 1.841\left[\left(\frac{2\pi\nu_o}{c}\right)^2 - \left(\frac{\pi}{L}\right)^2\right]^{-1/2} \qquad (3b)$$

where R is the cavity's radius, and ν_o is the alkali's 0-0 hyperfine transition frequency. Thus, alkali gas cell standards with high hyperfine transition frequencies are modelled as operating with appropriately smaller microwave cavities and resonance cells. Other general parameters used in the calculations are presented in Table II.

Table II. Parameters Used in the Calculation of the Clock Signal Shot Noise.

PARAMETER	VALUE
Laser Linewidth	50 MHz
Nitrogen Buffer Gas Pressure	10 torr
Photodetector Responsivity	0.5 amps/watt

III. RESULTS

The basic results of the calculations are presented in Fig. 1 and Table III. Clearly, Rb^{87} exhibits the best shot-noise-limited performance ($\sigma_y(\tau) = 5.4 \times 10^{-15}/\sqrt{\tau}$), and is roughly a factor of three better than any of the cesium isotopes. However, before saying too much about this result, one should note that the shot-noise-limited performance of the three cesium isotopes is a decreasing function of the isotope's hyperfine transition frequency. Given the equality of the nuclear spins of these isotopes, and the fact that the atomic line Q increases proportionate to ν_o, the result is counter-intuitive; typically, we would expect $\sigma_y(\tau) \sim 1/\nu_o$ under the condition of equal isotope nuclear spin.

Table III. Best Allan Deviations (i.e., Square Root of the Allan Variance) for the Various Candidate Alkalies as Well as the Corresponding Laser Intensity, Cell Temperature, and Peak Microwave Rabi Frequencies.

ALKALI	$\sigma_y^{best}(\tau)$	LASER INTENSITY $\mu W/cm^2$	TEMPERATURE °C	PEAK RABI FREQUENCY Hz	MINIMUM CAVITY VOLUME cm^3
^{85}Rb	$5.5 \times 10^{-15}/\sqrt{\tau}$	90	67	97	338.0
^{87}Rb	$5.4 \times 10^{-15}/\sqrt{\tau}$	128	73	155	29.6
^{133}Cs	$1.3 \times 10^{-14}/\sqrt{\tau}$	371	79	380	12.2
^{135}Cs	$1.4 \times 10^{-14}/\sqrt{\tau}$	291	78	309	10.3
^{137}Cs	$1.4 \times 10^{-14}/\sqrt{\tau}$	315	79	346	9.1

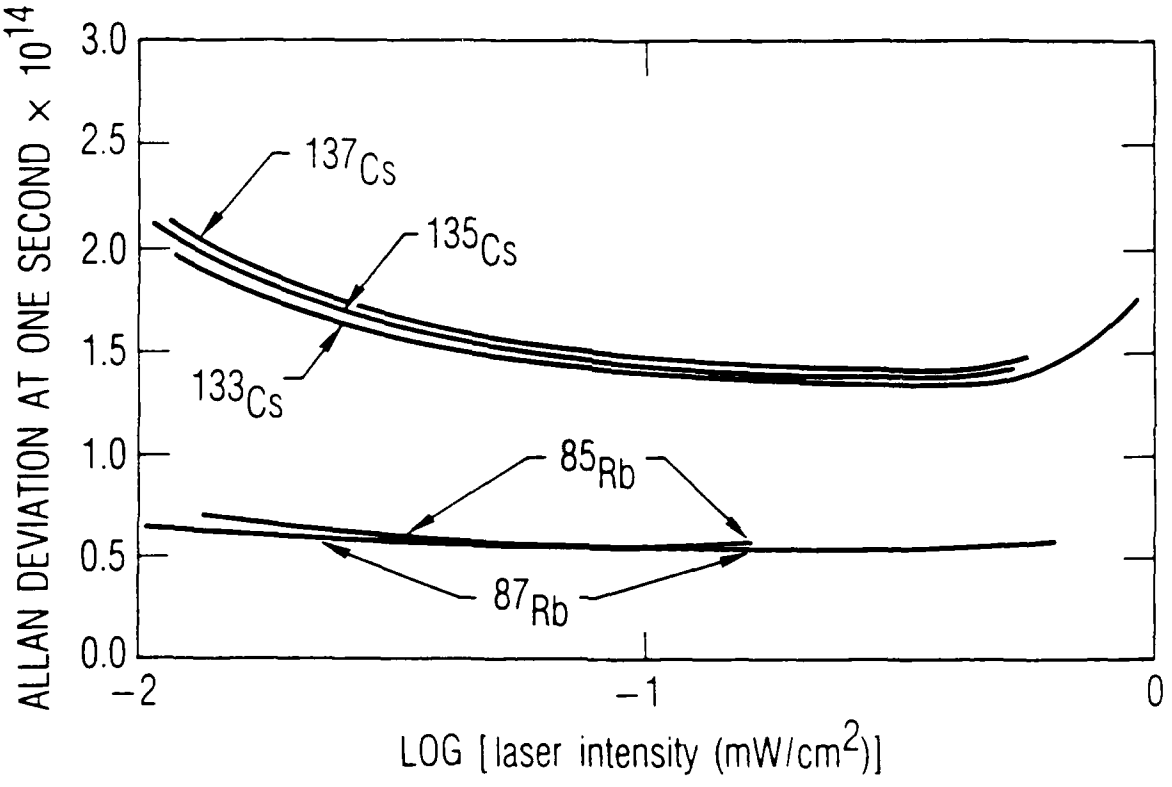

Fig. 1. Various Alkali Isotope Curves Showing the best Allan Deviations (i.e., Square Root of Allan Variance) as a Function of Incident Laser Intensity. Note that a Rb^{87} standard shows the best predicted performance. As discussed in the text the relation between the cesium isotope performances reflects the influence of cavity geometry on the Allan deviation, as well as intrinsic difference between the isotopes.

The resolution of this apparent paradox resides in the fact that these calculations assume a minimum volume microwave cavity, and hence a minimum volume resonance cell. As can be seen with the aid of Eq. (3) the cell volume decreases like $1/\nu_o^3$. Thus, the cesium isotope results can be explained by postulating a negative correlation between microwave cavity size and the shot-noise-limited Allan variance. This hypothesis has been substantiated by running the cesium isotope calculations for the fictitious case of equal cavity radii and lengths. The resulting Allan deviations scaled like $1/\nu_o$ (i.e., Cs^{137} showed a 10% improvement in shot-noise-limited performance compared to Cs^{133}). Consequently, the results presented in Fig. 1 and Table III not only represent the intrinsic performance capabilities of the various alkali isotopes, but also geometrical effects associated with the microwave cavity's size.

How the cavity geometry affects gas cell frequency standard performance is not understood at the present time. One possible explanation is that by increasing the microwave cavity length, and hence the resonance cell length, one obtains good transmitted light signal amplitudes at relatively low alkali densities. Since low alkali densities imply low spin-exchange rates, and hence relatively higher atomic Qs and signal-to-noise ratios, longer resonance cells might be expected to exhibit improved clock performance. In the same vein, because larger resonance cell radii imply lower phenomenological diffusional relaxation rates, one again might expect some improvement in predicted clock stability with larger radii resonance cells. An alternative explanation, however, is derived from the axial distribution of hyperfine polarization and microwave field strength in the resonance cell. Perhaps the influence of these distributions on clock signal amplitude is such that longer resonance cells yield relatively higher signal levels, and hence improved clock stability. In order to differentiate among these and other potential explanations for the influence of microwave cavity geometry on clock stability, additional calculations need to be performed, preferably with a more rigorous 3-dimensional model of the gas cell atomic frequency standard.

To mitigate the influence of cavity geometry on the calculation of shot-noise-limited performance, we considered the fictitious case of a Cs^{133} gas

cell frequency standard operating with a TE_{111} microwave cavity having the same radius and length as a Rb^{87} TE_{111} resonant cavity. Though the result of this calculation showed an improvement in clock stability compared to the Cs^{133} result given in table III, the best Allan deviation was nonetheless a factor of 1.6 larger than the corresponding Allan deviation of Rb^{87}. It would thus appear that the approximate factor of two difference in nuclear spins between Rb^{87} and Cs^{133} (i.e., the factor of two difference in the ground-state degeneracies) more than compensates for the 35% difference in the alkali ground state hyperfine splittings.

It is also surprising that Rb^{85} should display such good performance compared to Rb^{87}, considering that it has half the hyperfine resonance frequency and a 50% greater ground state degeneracy resulting from its larger nuclear spin. In light of the preceeding discussion of the Cs isotope Allan variances, we attribute this relatively good performance to Rb^{85}'s ten times larger minimum microwave cavity volume. This again emphasizes the influence of the physics package geometry on the ultimate shot-noise-limited performance that can be attained with the gas cell standard.

IV. SUMMARY

The present calculations indicate that a Rb^{87} gas cell standard shows the greatest potential for frequency stability, and in this regard nature has been uncommonly propitious. One should not, however, interpret this result as a superiority of the Rb^{87} standard in all regards. For example, if it is of primary importance to construct a miniature gas cell standard, then Cs^{133} might prove to be more advantageous given the fact that its minimum volume cavity occupies less than half the volume of a corresponding Rb^{87} cavity. Additionally, magnetic field sensitivities are less for Cs^{133} as a consequence of its greater hyperfine transition frequency. The only statement one should make regarding the present results is that of all the possible alkali gas cell standards that could be considered, a Rb^{87} standard appears to yield the best attainable shot-noise-limited performance.

REFERENCES

[1]. W. E. Bell, A. Bloom and R. Williams, "A Microwave Frequency Standard Employing Optically Pumped Sodium Vapor," IRE Trans. Microwave Theory Tech. MTT-7, pp. 95-98, (1959).

[2]. M. Arditi, "Frequency Control by Gas Cell Standards Fundamental Problems in the Light of Recent Experimental Results," Proc. 15th Annual Symp. on Freq. Control (Atlantic City, N.J., 31 May-2 June 1961) pp. 181-202.

[3]. G. Rovera, A. DeMarchi and J. Vanier, "The Optically Pumped Passive Cesium Frequency Standard: Basic Theory and Experimental Results on Buffer Gas Frequency Shifts," IEEE Trans. Instrum. Meas. IM-25, pp. 203-210, (1976).

[4]. G. Rovera, S. Leschiutta, G. Busca and F. Strumia, "Parameters Affecting the Stability of an Optically Pumped Cesium Frequency Standard," Proc. 32nd Annual Symp. on Freq. Control (Electronic Industries Assoc., Washington, D.C., 1978) pp. 466-468.

[5]. C. Audoin and J. Vanier, "Atomic Frequency Standards and Clocks," J. Phys. E 9, pp. 697-720, (1976).

[6]. J. Vanier, R. Kunski, P. Paulin, M. Tetu and N. Cyr, "On the Light Shift in Optical Pumping of Rubidium 87: The Techniques of 'Separated' and 'Integrated' Hyperfine Filtering," Can. J. Phys. 60, pp. 1396-1403, (1982).

[7]. L. L. Lewis and M. Feldman, "Optical Pumping by Lasers in Atomic Frequency Standards," Proc. 35th Annual Freq. Control Symp. (Electronic Industries Assoc., Washington, D.C., 1981), pp. 612-624.

[8]. G. Avila, E. deClercq, M. deLabachellerie and P. Cerez, "Microwave Ramsey Resonances From a Laser Diode Optically Pumped Cesium Beam Resonator," IEEE Trans. Instrum. Meas. IM-34, pp. 139-143, (1985).

[9]. J. C. Camparo, "The Diode Laser in Atomic Physics," Contemp. Phys. 26, pp. 443-477, (1985).

[10]. For an alkali-like atom of arbitrary nuclear spin I (i.e., either integer of half-integer) the equation describing the hyperfine splitting between two Zeeman sublevels ($|F=I+1/2=a, m\rangle - |F=I-1/2=b, n\rangle$) to second order in the magnetic field is:

$$\nu_{mn} = \nu_o + \frac{KB}{[I]}(m+n) + \frac{(KB)^2}{2\nu_o}\left(1 - \frac{(m^2+n^2)}{2[I]^2}\right)$$

where ν_o is the unperturbed hyperfine splitting, $K = g_j\mu_B/h = 2.80$ MHz/gauss, $[I]=(2I+1)$, and B is the magnitude of the static magnetic field. Clearly the transitions which, to first order, are insensitive to the magnetic field correspond to transitions where $m = -n$. However, as a consequence of the magnetic dipole selection rules, not all combinations of m and n yield allowed transitions. Specifically, we have the requirement that $\Delta m_F = m-n = 0, \pm 1$. Consequently, for any alkali-like atom the only magnetic field insensitive transitions which are allowed correspond to: i) $|a,0\rangle - |b,0\rangle$ or ii) $|a, \pm 1/2\rangle - |b, \mp 1/2\rangle$. Case i) corresponds to the well known 0-0 hyperfine transition occurring in half-integer species, while case ii) corresponds to alkali-like atoms with integer values of the nuclear spin. Therefore, one could base a gas cell clock on an integer nuclear spin alkali, but the stimulating microwave field would have to drive $\Delta m_F = \pm 1$ transitions rather than the traditional clock's $\Delta m_F = 0$ transition. To accomplish this would require a redesign of the microwave cavity configuration in the clock, and would present a series of difficulties and variations beyond the scope of the present study.

It should be noted, however, that from the above equation for ν_{mn} one can show that the $|a, \pm 1/2\rangle - |b, \mp 1/2\rangle$ transition frequencies are degenerate to second order in the magnetic field. Consequently, for a clock based on an I=1 alkali-like atom, four out of the six ground state Zeeman sublevels would contribute to the clock signal. This could result in a relative improvement in the clock's signal to noise ratio, and hence the clock's short term stability. Suffice it to say that gas cell frequency standards based on integer nuclear spin species may have potentially significant attributes.

We wish to thank the referee for pointing out the fact that integer nuclear spin alkalies can have field insensitive transitions, which stimulated us into rethinking the question of gas cell standards based on integer nuclear spin species.

[11] D. T. Goldman, in American Institute of Physics Handbook, edited by D. E. Gray (McGraw-Hill, New York, 1972), ch. 8b.

[12]. It might be argued that since the ground state hyperfine sublevels of Na^{23} are resolvable, this alkali isotope should be considered for further comparison. However, since the nuclear spins of Na^{23} and Rb^{87} are equal, and since the ground state hyperfine splitting of Rb^{87} is roughly four times greater than Na^{23}, the only possible advantage to a sodium standard would be in the very high optical pumping rates that can be achieved with dye lasers at the sodium resonance wavelengths. Since it was shown in Ref. 14 that optimum shot noise performance is achieved at relatively low optically pumping rates, it does not appear that high laser intensities at the Na^{23} first resonance wavelengths will mitigate against Na^{23} disadvantages: non-completely resolved hyperfine transitions and a small ground state hyperfine splitting.

[13]. J. C. Camparo and R. P. Frueholz, "A Nonempirical Model of the Gas-Cell Atomic Frequency Standard," J. Appl. Phys. 59, pp. 301-312, (1986).

[14]. J. C. Camparo and R. P. Frueholz, "Fundamental Stability Limits for the Diode Laser Pumped Rubidium Atomic Frequency Standard," J. Appl. Phys. 59, pp. 3313-3317, (1986).

[15]. J. C. Camparo and R. P. Frueholz, "Linewidths of the 0-0 Hyperfine Transition in Optically Pumped Alkali-Metal Vapors," Phys. Rev A 31, pp. 1440-1448, (1985).

[16]. J. C. Camparo and R. P. Frueholz, "Saturation of the 0-0 Hyperfine Transition Linewidth Enhancement Factor in Optically Pumped Alkali-Metal Vapors," Phys. Rev. A 32, pp. 1888-1889, (1985).

[17]. R. P. Frueholz and J. C. Camparo, "Microwave Field Strength Measurement in a Rubidium Clock Cavity Via Adiabatic Rapid Passage," J. Appl. Phys. 57, pp. 704-708, (1985).

[18]. H. E. Williams, T. M. Kwon and T. McClelland, "Compact Rectangular Cavity for Rubidium Vapor Cell Frequency Standards," Proc. 37th Annual Symp. on Freq. Control (IEEE Press, New York, 1983), pp. 12-17.

[19]. P. Minguzzi, F. Strumia and P. Violino, "Temperature Effects in the Relaxation of Optically Oriented Alkali Vapours," Nuovo Cimento 46B, pp. 145-161, (1966).

LABORATORY OPERATIONS

The Aerospace Corporation functions as an "architect-engineer" for national security projects, specializing in advanced military space systems. Providing research support, the corporation's Laboratory Operations conducts experimental and theoretical investigations that focus on the application of scientific and technical advances to such systems. Vital to the success of these investigations is the technical staff's wide-ranging expertise and its ability to stay current with new developments. This expertise is enhanced by a research program aimed at dealing with the many problems associated with rapidly evolving space systems. Contributing their capabilities to the research effort are these individual laboratories:

Aerophysics Laboratory: Launch vehicle and reentry fluid mechanics, heat transfer and flight dynamics; chemical and electric propulsion, propellant chemistry, chemical dynamics, environmental chemistry, trace detection; spacecraft structural mechanics, contamination, thermal and structural control; high temperature thermomechanics, gas kinetics and radiation; cw and pulsed chemical and excimer laser development including chemical kinetics, spectroscopy, optical resonators, beam control, atmospheric propagation, laser effects and countermeasures.

Chemistry and Physics Laboratory: Atmospheric chemical reactions, atmospheric optics, light scattering, state-specific chemical reactions and radiative signatures of missile plumes, sensor out-of-field-of-view rejection, applied laser spectroscopy, laser chemistry, laser optoelectronics, solar cell physics, battery electrochemistry, space vacuum and radiation effects on materials, lubrication and surface phenomena, thermionic emission, photosensitive materials and detectors, atomic frequency standards, and environmental chemistry.

Computer Science Laboratory: Program verification, program translation, performance-sensitive system design, distributed architectures for spaceborne computers, fault-tolerant computer systems, artificial intelligence, microelectronics applications, communication protocols, and computer security.

Electronics Research Laboratory: Microelectronics, solid-state device physics, compound semiconductors, radiation hardening; electro-optics, quantum electronics, solid-state lasers, optical propagation and communications; microwave semiconductor devices, microwave/millimeter wave measurements, diagnostics and radiometry, microwave/millimeter wave thermionic devices; atomic time and frequency standards; antennas, rf systems, electromagnetic propagation phenomena, space communication systems.

Materials Sciences Laboratory: Development of new materials: metals, alloys, ceramics, polymers and their composites, and new forms of carbon, nondestructive evaluation, component failure analysis and reliability; fracture mechanics and stress corrosion; analysis and evaluation of materials at cryogenic and elevated temperatures as well as in space and enemy-induced environments.

Space Sciences Laboratory: Magnetospheric, auroral and cosmic ray physics, wave-particle interactions, magnetospheric plasma waves; atmospheric and ionospheric physics, density and composition of the upper atmosphere, remote sensing using atmospheric radiation; solar physics, infrared astronomy, infrared signature analysis; effects of solar activity, magnetic storms and nuclear explosions on the earth's atmosphere, ionosphere and magnetosphere, effects of electromagnetic and particulate radiations on space systems; space instrumentation.

END

DATE

FILMED

5-88

DTIC